51st IEEE Conference on Decision and Control
December 10-13, 2012. Maui, Hawaii, USA

Periodic Adaptive Disturbance Observer for a Permanent Magnet Linear Synchronous Motor

Kwanghyun Cho[1], Jinsung Kim[1], Heeram Park[1], and Seibum Choi[2]

Abstract— **This paper proposes a periodic adaptive disturbance observer (PADOB) to control a PMLSM (Permanent Magnet Linear Synchronous Motor). The PADOB consists of a classical linear DOB and an adaptive mechanism which has been known as the periodic adaptive learning control (PALC). The key idea is to compensate parametric errors between the actual plant and the nominal model of DOB and disturbance forces such as the friction and detent force. The PADOB can improve the instability problem occurred by updating parameters of nominal model in the DOB directly. Through simulation test of the PMLSM, the validity of the PADOB is illustrated.**

I. INTRODUCTION

A Permanent Magnet Linear Synchronous Motor (PMLSM) has been used for works required accurate position or speed control. In PMLSMs, indirect coupling mechanisms such as chains, gear boxes and screw coupling are eliminated, and the effects of contact-types of nonlinearities and disturbances such as backlash and coupling frictional forces are reduced. Therefore, high-speed/high-accuracy positioning control is achieved perfectly.

However, it still exists the dominant disturbances such as the detent and friction force to be compensated. The detent force is occurred by the interaction between the permanent magnets and the steel teeth of the primary section. It is a position-dependent periodic disturbance and the pitch of permanent magnets becomes a period of the detent force.[1] The friction force is a velocity-dependent nonlinear disturbance. In most applications using PMLSMs, these disturbances have periodic and repetitive characteristics because required tasks are performed on the periodic trajectory under same conditions repetitively.

Numerous literatures have addressed about how to compensate these disturbances.[2] The detent force has been compensated by using a simple sinusoidal model because it can be represented as Fourier expansion. It estimates unknown parameters such as magnitude and phase of the sinusoidal model using certain parameter adaptation mechanisms.[3] However, it is not enough to eliminate one because it has not considered high order terms in the Fourier series for simplicity. The friction force also has been compensated by estimating parameters of friction model such as Coulomb friction model or Lugre friction model.[4][5] Here, the friction coefficients are assumed to be constants while nonlinearities such as deadzone, hysteresis, and saturation are ignored. Although a model considered high order harmonics terms and nonlinearities is used, it is difficult to prove asymptotically convergence of estimated parameters. On the other hand, parameter convergence is not required in disturbance observer (DOB).[6] It eliminates the output of inverse nominal model considered as external disturbances which are mostly the detent and friction force. However, it is very dependent on parameters of the nominal model. Therefore, above mentioned schemes are extremely constrictive to the used model.

To improve these problems, the learning control strategies without the model have been suggested, which have been known as the periodic adaptive learning control (PALC). [7][8][9][10][11] Adaptive learning compensators of these disturbances in PMLM were designed in [7]. The key idea is to use the state-periodic characteristics of these disturbances, which are a position-dependent detent force and a velocity-dependent friction force. The past information of more than one period along the state axis is used to update the current adaptation learning law. It means that initial conditions of the estimated disturbances are required to update the current information of these disturbances. Therefore, certain adaptive scheme or nonlinear functions must be designed additionally and it can be very complicated.

In this paper, a periodic adaptive disturbance observer (PADOB) is proposed. The classical linear DOB is used to design initial conditions in adaptation laws, which include parametric errors between the actual plant and nominal model and external disturbances such as detent and friction force. And the PALC is used to update and compensate these disturbances. Therefore, the proposed PADOB can improve the instability problem occurred by updating parameters of nominal model directly in the DOB. Also, it can improve complicated procedures to design the initial conditions in PALC.

This paper is organized as follows: In Section II, the used PMLSM model and control problem are introduced. In Section III, the proposed PADOB are presented. The simulation illustration is shown in Section IV to verify the performance of PADOB. Concluding remarks are given in Section V.

II. PROBLEM FORMULATION

In this section, the PMLSM model and control problem are formulated. Also, the properties of PALC are presented.

[1]K. Cho, J. Kim and H. Park are with the Department of Mechanical Engineering, KAIST, 335 Gwahak-ro (373-1 Guseong-dong), Yuseong-gu, Daejeon, 305-701, Republic of Korea khcho08@kaist.ac.kr, jsk@kaist.ac.kr, hrpark@kaist.ac.kr

[2]S.B. Choi is with the faculty of the Department of Mechanical Engineering, KAIST, 335 Gwahak-ro (373-1 Guseong-dong), Yuseong-gu, Daejeon, 305-701, Republic of Korea sbchoi@kaist.ac.kr

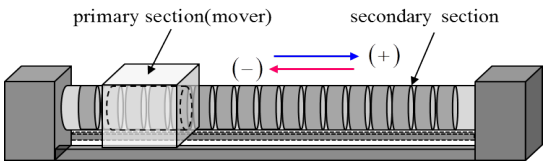

Fig. 1. Permanent Magnet Linear Synchronous Motor

A. PMLSM Model

The PMLSM is depicted in Fig. 1 and it is represented by the dynamic equation as follows, [7]

$$m\ddot{x}(t) = -\frac{k_f k_e}{R}\dot{x}(t) + \frac{k_f}{R}v(t) - F_{det}(x) - F_{fric}(\dot{x}) \quad (1)$$

where, x is the position of the primary section, m the mass of the primary section, k_f the force constant, k_e the back-emf constant, R the resistance, $v(t)$ the input voltage, F_{det} the detent force, and F_{fric} the friction force. For simplicity, the load and small external disturbance are ignored.

The control objective is to track the given desired position, x_d and the corresponding desired velocity, $\dot{x}_d$ with tracking error as small as possible. The performed task is assumed as follows:

Assumption 1: The task is performed on the periodic trajectory under same conditions repetitively.

Assumption 2: The disturbance effects are nearly identical when the primary section moves to the positive direction and negative direction because of good tracking performance.

Assumption 3: The measurement noise and high frequency disturbance are attenuated by low pass filters.

Suppose that the detent force is described as a nonlinear functions and the friction force is presented as a sign function such as follows,

$$F_{det}(x) = a(x), \quad F_{fric}(\dot{x}) = b(t)sgn(\dot{x})$$

The equation of the PMLSM, (1) is rewritten as follows:

$$M\ddot{x}(t) = -B\dot{x}(t) + u(t) - a(x) - b(t)sgn(\dot{x}) \quad (2)$$

where, M is the mass of the primary section ($M := m$), $u(t)$ the control input $\big(u(t) := k_f/R \cdot v(t)\big)$, and B defines as the viscous friction coefficient ($B := k_f k_e/R$).

B. Properties of PALC

In this section, the defined properties of PALC are introduced, which are applied to the proposed PADOB.

Property 1: (Total pass trajectory)
The total passed trajectory is given as follows,

$$x_s(t) = \int_0^t \frac{|dx|}{d\tau}d\tau = \int_0^t |v(\tau)|d\tau$$

where, x is the position, and v the velocity. Since x_s is the summation of absolute position increase along the time axis, it is a monotonously growing signal. Physically it is the total passed trajectory; hence, it has the following property:

$$x_s(t_1) \geq x_s(t_2), \quad iff \quad t_1 \geq t_2$$

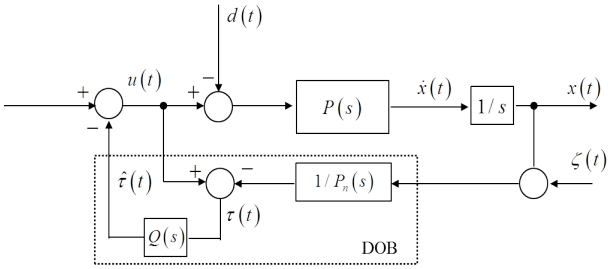

Fig. 2. Classical linear DOB structure

Property 2: (Trajectory periodicity)
From Assumption 1, the passed position has a periodicity on the total passed trajectory:

$$x(t) = x_s(t) - m' x_{s_p}$$

where, x is the position, x_{s_p} the moving distance for a period and m' the integer part of $x_s(t)/x_{s_p}$. When it assumes that the tracking performance is good, the position and velocity can be presented in time-domain as follows,

$$x(x_s) = x(x_s - x_{s_p}) \quad \rightarrow \quad x(t) = x(t - P_t), \quad \dot{x}(t) = \dot{x}(t - P_t)$$

where, P_t is a time period of performed task.

Property 3: (Disturbance periodicity)
From Assumption 2 and Property 2, the detent and friction force have the following properties:

$$a(t) = a(t - P_t)$$

$$b(t)sgn(\dot{x}(t)) = b(t - P_t)sgn(\dot{x}(t - P_t))$$

III. PERIODIC ADAPTIVE DISTURBANCE OBSERVER

A. Disturbance Observer

The DOB has been proposed to eliminate the disturbance which is difference between the actual system and nominal model. The nominal model represents the desired model based on the desired control specifications. It makes the actual system to become a given nominal model. Fig. 2 depicts the classical linear DOB structure. The output of DOB, $\hat{\tau}(t)$ is an estimated disturbance which consists of the parametric errors between the actual plant and the nominal model of DOB and disturbance forces such as friction and detent force. The symbols in Fig. 2 are defined as follows,

$x(t)$, $\dot{x}(t)$: the position and velocity of mover
P(s), P_n(s): the transfer function of actual, nominal plant
$u(t)$: the control input
$d(t)$: the disturbance including detent and friction force
$Q(s)$: a low-pass filter
$\tau(t)$: the estimated disturbance without filtering
$\hat{\tau}(t)$: the estimated disturbance with a low-pass filter
$\zeta(t)$: the measurement noise

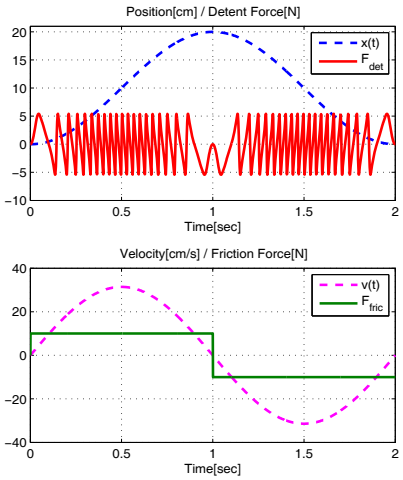

Fig. 3. Disturbance Characteristics

The transfer functions and disturbance are presented as follows,

$$P(s) = 1/(Ms+B) \tag{3}$$

$$P_n(s) = 1/(M_n s+B_n) \tag{4}$$

$$d(t) = a(x)+b(t)sgn(\dot{x}) \tag{5}$$

where, M_n and B_n are nominal values of the nominal model. The output of the plant, $x(t)$ is represented by

$$x(t) = \frac{PP_n}{D}u_r(t)+\frac{PP_n(1-Q)}{D}d(t)-\frac{PQ}{D}\zeta(t) \tag{6}$$

where, $D = 1/\big(P_n+(P-P_n)Q\big)$.

Assume that the transfer functions in (6) are stable. In the low frequency range(i.e., $Q(j\omega)\approx 1$), the output $x(j\omega)$ becomes similar to $P_n(j\omega)u_r(j\omega)-\zeta(j\omega)$, but from Assumption 3($\zeta\approx 0$), we have the nominal input-output relation, i.e., $x(j\omega)\approx P_n(j\omega)u_r(j\omega)$, which is desired. More detailed DOBs are presented in numerous literatures.[12][13]

B. PADOB

The DOB has been known as a powerful scheme as referred to numerous literatures. However, in case that parameters of nominal model are inaccurate, the performance can be worse. Therefore, the information of nominal model must be updated. To update parameters of the nominal model directly can occur instability problems because poles and zeros of the transfer function of nominal model are changed. This paper has focused on updating not parameters of nominal model, M and B but output of DOB, τ(t).

1) Disturbance Decomposition: In this section, the output of DOB is calculated to decompose disturbances and use them as initial conditions of the periodic adaptation mechanism. In Fig. 2, the estimated disturbance without filtering can be presented as follows,

$$\tau(t) = u(t)-\frac{1}{P_n(s)}(x(t)+\zeta(t)) \tag{7}$$

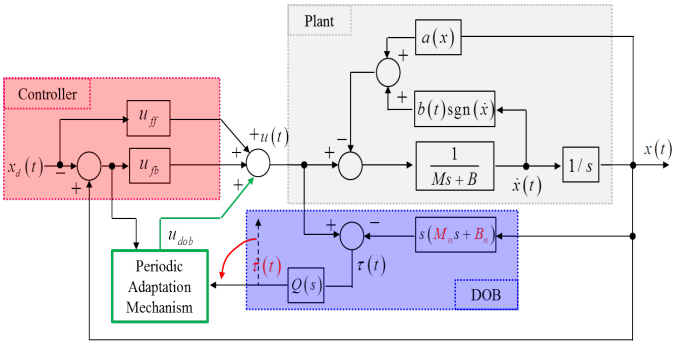

Fig. 4. Periodic Adaptive DOB structure

For simplicity, variables in time-domain and s-domains are used simultaneously. Substituting (4) into (7),

$$\tau(t) = u(t)-M_n\ddot{x}(t)-B_n\dot{x}(t) \tag{8}$$

where, ζ=0 by Assumption 3.

And the output of the transfer function of the actual plant is presented as follows,

$$x(t) = \frac{1}{Ms^2+Bs}\big(u(t)-d(t)\big) \tag{9}$$

Rearranging (9), the control input, $u(t)$ is rewritten as follows,

$$u(t) = d(t)+M\ddot{x}(t)+B\dot{x}(t) \tag{10}$$

Substituting (5) and (10) into (8), the estimated disturbance can be presented as follows,

$$\tau(t) = \Delta M\ddot{x}(t)+\Delta B\dot{x}(t)+a(x)+b(t)sgn(\dot{x}) \tag{11}$$

where, the inertia error is $\Delta M = M-M_n$ and the viscous friction coefficient error is $\Delta B = B-B_n$.

From Assumption 1 and 2, the detent and friction force can be described in Fig. 3 as an example. When the desired trajectory is given as one in Fig. 3, the detent and friction force become an even and odd function. Also, the inertia error and viscous friction coefficient error become an even and odd function depending on states such as position and velocity. Therefore, the state-dependent disturbances can be decomposed as follows,

$$\Delta M\ddot{x}(t)+a(x) = \frac{1}{2}\big[\tau(t)+\tau(P_t-t)\big] \tag{12}$$

$$\Delta B\dot{x}(t)+b(t)sgn(\dot{x}) = \frac{1}{2}\big[\tau(t)-\tau(P_t-t)\big] \tag{13}$$

where, P_t is the time period which a task is performed.

2) Periodic Adaptation Mechanism and Controller: The structure of PADOB is described in Fig. 4. The system is controlled by following two step:

- When $x_s < 2x_{s_p}$, the system is controlled by using the classical linear DOB to be bounded input bounded output(BIBO).
- When $x_s \geq 2x_{s_p}$, the system is controlled by the proposed PADOB. By the periodic adaptation mechanism, the unknown disturbances are estimated.

First, consider the case when $x_s < 2x_{s_p}$. The control law is designed as follows:

$$\begin{aligned} u_1(t) &= u_{fb_1}(t) + u_{ff_1}(t) \\ u_{fb_1}(t) &= -K_0 S(t) - M_n \lambda \dot{e}_x(t) \\ u_{ff_1}(t) &= M_n \ddot{x}_d(t) + B_n \dot{x}_d(t) \end{aligned} \tag{14}$$

where,

$$S(t) = \dot{e}_x(t) + \lambda e_x(t), \qquad e_x(t) = x(t) - x_d(t)$$

x_d is the desired position, K_0 and λ are tuning parameter ($K_0 > 0$, $\lambda > 0$).

Substituting (14) into (2), the closed-loop error dynamics are obtained as follows,

$$\begin{aligned} &M\ddot{e}_x(t) + B\dot{e}_x(t) + M_n\lambda\dot{e}_x(t) + K_0 S(t) \\ &\quad = -[\Delta M \ddot{x}_d(t) + \Delta B \dot{x}_d(t) + a(x) + b(t)sgn(\dot{x})] \end{aligned} \tag{15}$$

In (15), the effect of the inner-loop compensator (DOB) is ignored because it forces the system to be stable. And the desired trajectories, $x_d(t)$, $\dot{x}_d(t)$, and $\ddot{x}_d(t)$ are bounded in practice. Also, assuming that $|\Delta M|$, $|\Delta B|$, and $|a(x) + b(t)sgn(\dot{x})|$ are all bounded, the system satisfies the BIBO stable.

Next, consider the case when $x_s \geq 2x_{s_p}$. The designed control law is as follows,

$$\begin{aligned} u_2(t) &= u_{fb_2}(t) + u_{ff_2}(t) + u_{PADOB}(t) \\ u_{fb_2}(t) &= -K_0 S(t) - M_n \lambda \dot{e}_x(t) + B_n \dot{x}(t) \\ u_{ff_2}(t) &= M_n \ddot{x}_d(t) \\ u_{PADOB}(t) &= \hat{a}_M(t) + \hat{b}_B(t) \end{aligned} \tag{16}$$

And, the adaptation laws of $u_{PADOB}(t)$ are designed as follows,

$$\hat{a}_M(t) = \begin{cases} \hat{a}_M(t-P_t) - K_1 S(t) & if \quad x_s \geq 2 \cdot x_{s_p} \\ \hat{a}_{M0}(t) & if \quad 0 < x_s < 2 \cdot x_{s_p} \end{cases} \tag{17}$$

$$\hat{b}_B(t) = \begin{cases} \hat{b}_B(t-P_t) - K_2 S(t) & if \quad x_s \geq 2 \cdot x_{s_p} \\ \hat{b}_{B0}(t) & if \quad 0 < x_s < 2 \cdot x_{s_p} \end{cases} \tag{18}$$

where,

$$\hat{a}_M(t) = \hat{a}(t) + \Delta\hat{M}\ddot{x}(t), \quad \hat{b}_B(t) = \hat{b}(t)sgn(\dot{x}(t)) + \Delta\hat{B}\dot{x}(t)$$

Here, K_1 and K_2 are adaptation gains ($K_1 > 0$, $K_2 > 0$).

The initial conditions of the disturbances, $\hat{a}_{M0}$ and $\hat{b}_{B0}$ are obtained by the output of DOB, (12) and (13). The control input, (16) and adaptation laws, (17), (18) guarantee that the system is asymptotically stable. The Lyapunov stability analysis is performed to prove it.

Consider the following positive Lyapunov candidate function at $s(t)$, whose corresponding time is t:

$$\begin{aligned} V(s(t)) = V(t) = \frac{1}{2}S(t)^2 &+ \frac{1}{2K_1M_n}\int_{t-P_t}^{t} {e_{aM}}^2(\tau)d\tau \\ &+ \frac{1}{2K_2M_n}\int_{t-P_t}^{t} {e_{bB}}^2(\tau)d\tau \end{aligned} \tag{19}$$

where,

$$\begin{aligned} e_{aM}(t) &= e_a + e_{\Delta M}\ddot{x}(t), \quad & e_{bB}(t) &= e_b sgn(\dot{x}(t)) + e_{\Delta B}\dot{x}(t) \\ e_a(t) &= a(t) - \hat{a}(t), \quad & e_b(t) &= b(t) - \hat{b}(t) \\ e_{\Delta M}(t) &= \Delta M(t) - \Delta\hat{M}(t), \quad & e_{\Delta B}(t) &= \Delta B(t) - \Delta\hat{B}(t) \end{aligned}$$

Then, the difference of the positive Lyapunov candidate functions at two discrete time point (t and $t - P_t$) can be calculated as:

$$\begin{aligned} \Delta V =& V(t) - V(t-P_t) = \frac{1}{2}S^2(t) - \frac{1}{2}S^2(t-P_t) \\ &+ \frac{1}{2K_1M_n}\int_{t-P_t}^{t}\left[{e_{aM}}^2(\tau) - {e_{aM}}^2(\tau-P_t)\right]d\tau \\ &+ \frac{1}{2K_2M_n}\int_{t-P_t}^{t}\left[{e_{bB}}^2(\tau) - {e_{bB}}^2(\tau-P_t)\right]d\tau \end{aligned} \tag{20}$$

For simplicity, let the first term on the right hand side be denoted by A, the second integral term by B, and the third integral term by C. Then, A is calculated as follows,

$$\begin{aligned} A =& \frac{1}{2}S^2(t) - \frac{1}{2}S^2(t-P_t) = \int_{P_t}^{t} S(\tau)\dot{S}(\tau)d\tau \\ =& \int_{t-P_t}^{t}\frac{1}{M_n}\left[-e_{aM}(\tau)S(\tau) - e_{bB}(\tau)S(\tau) - K_0S^2(\tau)\right]d\tau \end{aligned} \tag{21}$$

For a proof, see the appendix.

And, based on Property 1 and 3, the following equalities are satisfied:

$$a_M(t) = a_M(t-P_t) \tag{22}$$

$$b_B(t) = b_B(t-P_t) \tag{23}$$

Then, using (22), B can be calculated as follows,

$$\begin{aligned} B =& \frac{1}{2K_1M_n}\int_{t-P_t}^{t}\left[{e_{aM}}^2(\tau) - {e_{aM}}^2(\tau-P_t)\right]d\tau \\ =& \frac{1}{2K_1M_n}\int_{t-P_t}^{t}\left[a_M(\tau) - \hat{a}_M(\tau)\right]^2 \\ &\qquad - \left[a_M(\tau-P_t) - \hat{a}_M(\tau-P_t)\right]^2 d\tau \\ =& \frac{1}{2K_1M_n}\int_{t-P_t}^{t}\left[\hat{a}_M(\tau-P_\tau - \hat{a}_M(\tau)\right] \\ &\cdot \left\{2\left[a_M(\tau) - \hat{a}_M(\tau)\right] + \left[\hat{a}_M(\tau) - \hat{a}_M(\tau-P_\tau)\right]\right\}d\tau \\ =& \frac{1}{2K_1M_n}\int_{t-P_t}^{t}\alpha(\tau)\cdot\left\{2e_{aM}(\tau) - \alpha(\tau)\right\}d\tau \end{aligned} \tag{24}$$

where,

$$\alpha(\tau) = \hat{a}_M(\tau-P_\tau) - \hat{a}_M(\tau)$$

Also, using (23), C can be obtained as follows,

$$\begin{aligned} C =& \frac{1}{2K_2M_n}\int_{t-P_t}^{t}\left[{e_{bB}}^2(\tau) - {e_{bB}}^2(\tau-P_t)\right]d\tau \\ =& \frac{1}{2K_2M_n}\int_{t-P_t}^{t}\left[b_B(\tau) - \hat{b}_B(\tau)\right]^2 \\ &\qquad - \left[b_B(\tau-P_t) - \hat{b}_B(\tau-P_t)\right]^2 d\tau \\ =& \frac{1}{2K_2M_n}\int_{t-P_t}^{t}\left[\hat{b}_B(\tau-P_\tau - \hat{b}_B(\tau)\right] \\ &\cdot \left\{2\left[b_B(\tau) - \hat{b}_B(\tau)\right] + \left[\hat{b}_B(\tau) - \hat{b}_B(\tau-P_\tau)\right]\right\}d\tau \\ =& \frac{1}{2K_2M_n}\int_{t-P_t}^{t}\beta(\tau)\cdot\left\{2e_{bB}(\tau) - \beta(\tau)\right\}d\tau \end{aligned} \tag{25}$$

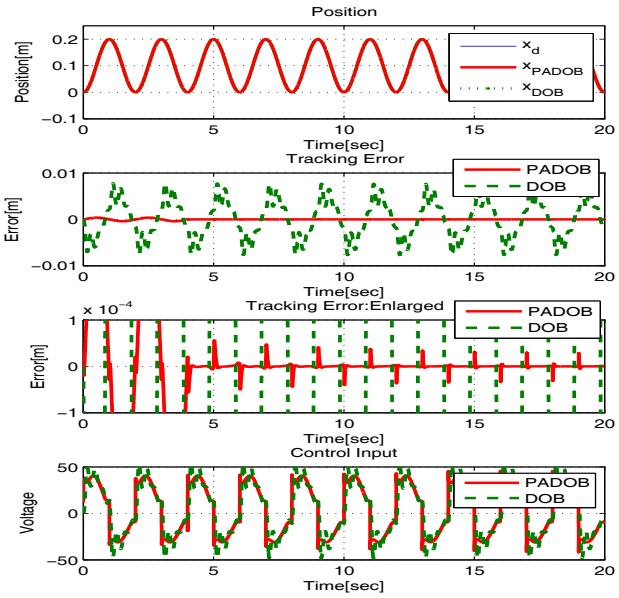

Fig. 5. Case1: $M_n = M$ and $B_n = B$

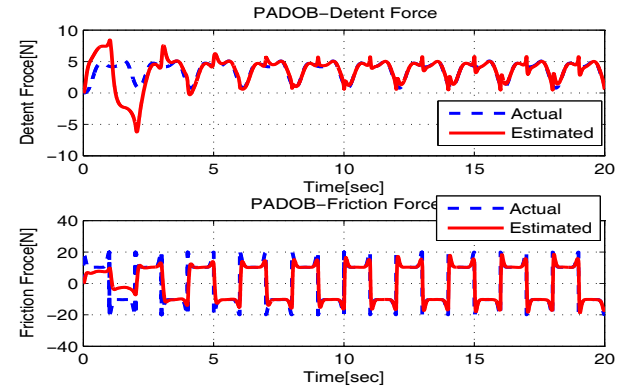

Fig. 6. Case1: detent and friction force

where,

$$\beta(\tau) = \hat{b}_B(\tau - P_\tau) - \hat{b}_B(\tau)$$

Substituting (16), (17) and (18) into (21), (24) and (25), (20) is rewritten as follows,

$$\begin{aligned}\Delta V =& A + B + C \\ =& \int_{t-P_t}^{t} -\frac{1}{M_n} K_0 S^2 - \frac{K_1}{2M_n} S^2 - \frac{K_2}{2M_n} S^2 d\tau \\ =& \int_{t-P_t}^{t} -\frac{1}{M_n}\left(K_0 + \frac{K_1}{2} + \frac{K_2}{2}\right) S^2 d\tau \end{aligned} \quad (26)$$

The difference of the Lyapunov candidate function becomes $\Delta V(t) \leq 0$. From LaSalle's invariant set theorem, the asymptotical stability is proved. From (26), only $S = 0$ makes $\Delta V = 0$. Using the $S(t) = \dot{e}_x + \lambda e_x$, if $e_x(0) = 0$, only $e_x = 0$ makes $S = 0$. Also, since $e_x = 0$, we have $\dot{e}_x = 0$. Therefore, e_x and $\dot{e}_x$ are asymptotically stable at equilibrium points.

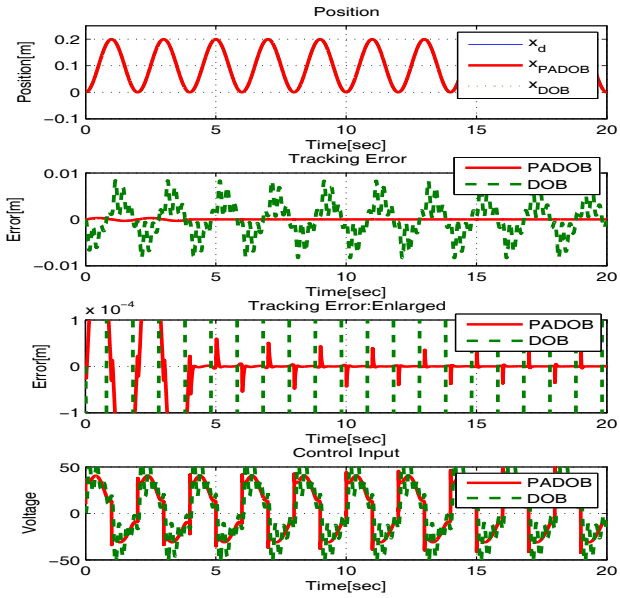

Fig. 7. Case2: $M_n = 10$ and $B_n = 60$

IV. SIMULATION ILLUSTRATIONS

The simulation tests have been performed to verify the performance of PADOB. The results are compared with one of PI controller with a classical linear DOB.

For the simulation test, the following reference trajectory is used:

$$x_d(t) = 0.1 - 0.1 \cdot \cos(\pi t)$$

The friction force is modelled as follows:

$$F_{fric}(\dot{x}) = \left\{10 + 10exp(-\dot{x}/0.1)^2) + abs(\dot{x})\right\} sgn(\dot{x})$$

And, the detent force is modelled as follows:

$$\begin{aligned} F_{det}(x) =& 4\sin(\frac{2\pi x}{T_c}) + 2\sin(\frac{4\pi x}{T_c}) + \sin(\frac{6\pi x}{T_c}) \\ &+ 0.5\sin(\frac{8\pi x}{T_c}) + 0.25\sin(\frac{10\pi x}{T_c}) + 0.125\sin(\frac{12\pi x}{T_c}) \end{aligned}$$

where, T_c is the pitch of the permanent magnet. The parameters of actual plant are $M = 12kg$, and $B = 72.38N/m/s$. The performed simulation cases are shown as follows:

- Case 1 (Fig. 5, 6): M_n = 12 and B_n = 72.68
- Case 2 (Fig. 7, 8): M_n = 10 and B_n = 60.00

In Fig 5 and 7, the tracking performance of PADOB is superior than one of PI controller with DOB. The tracking error has become smaller and smaller as time goes on. It shows that disturbances have been updated as shown in Fig 6 and 8. And, Case 2 shows that the PADOB has a better performance than the PI controller with DOB although parametric errors exist in the nominal model. The performance of PI controller with DOB becomes worse if the control gain make be higher to reduce the tracking error because it occurs

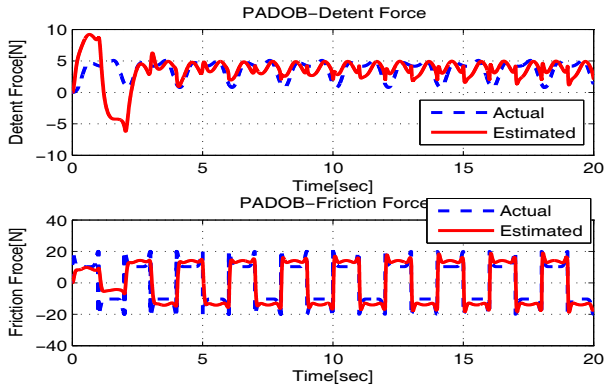

Fig. 8. Case2: detent and friction force

serious chattering of the control input. Therefore, test results show that the performance of PADOB is superior.

V. CONCLUSION

In this paper, a periodical adaptive disturbance observer (PADOB) was developed which consists of periodic adaptive learning control (PALC) and a classical linear DOB. The key idea of PADOB is to make use of the output of DOB as initial conditions for PALC. Therefore, the instability problem was improved by updating the output of DOB and the performance of DOB was higher. Also, the complicated procedures to design initial conditions in PALC were reduced by decomposition of disturbances of DOB based on periodic characteristics. From simulation results, it is shown that the PADOB provides a superior tracking performance. However, the performance of PADOB can be restricted by Q-filter. As future works, the effect of Q-filter (LPF) must be studied.

APPENDIX

In this appendix, we prove (21),

$$A = \frac{1}{2}S^2(t) - \frac{1}{2}S^2(t-P_t) = \int_{P_t}^{t} S(\tau)\dot{S}(\tau)d\tau$$
$$= \int_{t-P_t}^{t} \frac{1}{M_n}\left[-e_{aM}S(t) - e_{bB}S(t) - K_0S^2(t)\right]d\tau$$

Here, $\dot{S}(t)$ is calculated as follows,

$$\begin{aligned}
\dot{S}(t) =& \ddot{e}_x + \lambda\dot{e}_x = (\ddot{x} - \ddot{x}_d) + \lambda\dot{e}_x \\
=& \frac{1}{M}\{-B\dot{x} + u(t) - a(x) - b(t)sgn(\dot{x})\} - \ddot{x}_d + \lambda\dot{e}_x \\
=& \frac{1}{M}\{-B\dot{x} - K_0S(t) - M_n\lambda\dot{e}_x(t) + B_n\dot{x}(t) + M_n\ddot{x}_d(t) \\
& + \hat{a}(t) + (\Delta M\ddot{x} - \Delta M\ddot{x}) + \Delta\hat{M}\ddot{x} + \hat{b}(t)sgn(\dot{x}) + \Delta\hat{B}\dot{x} \\
& - a(x) - b(t)sgn(\dot{x})\} - \ddot{x}_d + \lambda\dot{e}_x \\
=& \frac{1}{M}\{-B\dot{x} - \Delta M\ddot{x} - a(x) - b(t)sgn(\dot{x}) + \Delta\hat{M}\ddot{x} - K_0S(t) \\
& + \Delta\hat{B}\dot{x} + \Delta M\ddot{x} + \hat{a}(t) + \hat{b}(t)sgn(\dot{x}) - \Delta M\ddot{x}_d + \Delta M\lambda\dot{e}_x\} \\
=& \frac{1}{M}\{-e_{\Delta B}\dot{x} - e_{\Delta M}\ddot{x} - e_a - e_bsgn(\dot{x}) - K_0S(t) + \Delta M\dot{S}\} \\
=& \frac{1}{M}\{-e_{bB} - e_{aM} - K_0S(t) + \Delta M\dot{S}\} \qquad (27)
\end{aligned}$$

Rearranging (27),

$$(1 - \Delta M/M)\dot{S} = (1/M)\{-e_{bB} - e_{aM} - K_0S(t)\} \qquad (28)$$

From (28), $\dot{S}(t)$ can be presented as follows,

$$\dot{S} = (1/M_n)\{-e_{bB} - e_{aM} - K_0S(t)\} \qquad (29)$$

Therefore, A is obtained by substituting (29) into (21).

ACKNOWLEDGMENT

This work was supported by the National Research Foundation of Korea (NRF) grant funded by the Korea goverment(MEST), (No.2012-0000991).

REFERENCES

[1] AW van Zyl and C. Landy, "Reduction of cogging forces in a tubular linear synchronous motor by optimizing the secondary design", *in 2002 IEEE AFRICON*, Oct. 2002, pp. 689-692.
[2] S. Chen, "Modeling and Compensation of Ripples and Friction in Permanent-Magnet Linear Motor Using a Hysteretic Relay", *IEEE/ASME Trans. Mechatronics*, vol. 15, no. 4, pp. 586-594, 2010
[3] K. Tan and et al., "Robust Adaptive Numerical Compensation for Friction and Force Ripple in Permanent-Magnet Linear Motors", *IEEE Trans. Magnetics*, vol. 38, no. 1, pp.221-228, 2002
[4] L. Marton and B. Lantos, "Modeling, Identification, and Compensation of Stick-Slip Friction", *IEEE Trans. Industrial Electronics*, vol. 54, no. 1, pp.511-521, Feb 2007
[5] L. Lu and et al., "Adaptive Robust Control of Linear Motors with Dynamic Friction Compensation using Modified LuGre Model", *Automatica*, vol. 45, no. 12, pp.2890-2896, 2009
[6] M. Yan and Y. Shiu, "Theory and Application of a Combined Feedback-Feedforward Control and Disturbance Observer in Linear Motor Drive Wire-EDM Machines", *International Journal of Machine Tools and Manufacture*, vol. 48, no. 3-4, pp.388-401, 2008
[7] H. Ahn, Y. Chen and H. Dou, "State-periodic Adaptive Cogging and Friction Compensation of Permanent Magnetic Linear Motors", *IEEE Trans. Magnetics*, vol. 41, no. 1, pp.90-98, 2005
[8] H. Ahn and Y. Chen, "State-dependent Periodic Adaptive Disturbance Compensation", *IET Control Theory and Applications*, vol. 1, no. 4, pp.1008-1014, 2007
[9] H. Ahn and Y. Chen, "State-dependent Friction Force Compensation Using Periodic Adaptive Learning Control", *Mechatronics*, vol. 19, no. 6, pp.896-904, 2009
[10] H. Ahn and Y. Chen, "Periodic Adaptive Learning Compensation of State-dependent Disturbance", *IET Control Theory and Applications*, vol. 4, no. 4, pp.529-538, 2010
[11] H. Ahn, K. Moore and Y. Chen, "Trajectory-keeping in Satellite Formation Flying via Robust Periodic Learning Control", *Int. J. Robust and Nonlinear Control*, vol. 20, no. 14, pp.1655-1666, 2010
[12] M. Tomizuka, "Model Based Prediction, Preview and Robust Controls in Motion Control Systems", *Proc. of Int. Workshop on Advanced Motion Control*, pp.1-6, 1996
[13] T. Umeno and Y. Hori, "Robust Speed Control of DC Servomotors using Modern Two Degrees-of-freedom Controller Design", *IEEE Trans. Industrial Electronics*, vol. 38, pp.363-368, 1991